ABSORPTIVE EFFECTS IN PERIPHERAL PRODUCTION PROCESSES: THE REACTION $\bar{p}p \to \overline{N^*}N^*$

B.E.Y. Svensson
CERN - Geneva

A B S T R A C T

The production of N*(1237), the nucleon $3/2 - 3/2^+$ isobar, in pair with its antiparticle in proton - antiproton collisions in the laboratory momentum range 3.25 - 7 GeV/c is considered in the one-pion exchange model, modified to take into account absorption in the initial and final state due to competition from other open channels according to the theory by Gottfried and Jackson. It is found that this model reproduces well the slope of the differential cross - section, the decay distribution, including an observed small correlation in the decay of the isobar and the anti - isobar, and the energy dependence of the cross-section, although the absolute magnitude of the cross - section is about a factor of five too big. The production of Y*(1382) and its antiparticle from the same initial state is also briefly discussed.

65/657/5-TH.549
6 April 1965

1. INTRODUCTION

The theoretical model usually applied in analysing quasi-two-body resonance production (we call a particle, unstable with respect to strong interaction, a resonance) is the one-meson exchange model (OMEM)[1]. Due to the spins of the particles involved, however, this model fails, in general, to reproduce the experimentally observed concentration to small production angles, a fact which is connected to the observation that the unmodified OMEM usually exceeds the unitarity limit in the low partial waves[2]. One argues, anyhow, that the main idea of this model is right, partly because of its success in predicting resonance decay distributions.

One is then faced with the problem of modifying the simple OMEM in some way, in order to have it reproducing the peripheral production experimentally found. The modifications suggested so far fall mainly into one of the following three categories:

a) Inclusion of form factors or other "off-shell" corrections[1,3,4]. We refer to this approach as the form factor version of the OMEM.

b) Inclusions of effects due to competition from other open channels, based on the analogy to the distorted wave Born approximation (DWBA) of nuclear physics[2,5,6]. We refer to this approach as the absorption model, because it lumps all the other open channels together and treats them as being absorbed.

c) Explicit unitarization, e.g., by means of the K-matrix[7].

In this paper we study the reaction

$$\bar{p}p \to \overline{N^{*++}}\, N^{*++} \qquad (1)$$

where N^* is the pion-nucleon $3/2 - 3/2^+$ resonance of mass 1237 MeV and width 125 MeV[8], under the assumption that the reaction takes place mainly through one-pion exchange, which is modified according to the absorption model. We devote Section 2 to some general considerations concerning helicity amplitudes, cross-section and decay distributions for reaction (1), followed by a list of formulae for these quantities in the Born approximation.

The necessary concepts of the absorption model are described in Section 3; it is then applied to reaction (1) in Section 4. The comparison with experiment is given in Section 5, while Section 6 briefly treats the reaction

$$\bar{p}p \to \bar{Y}^{*+} Y^{*+} , \qquad (2)$$

where Y* is the $\Lambda - \pi$ resonance of mass 1382 MeV and width 53 MeV[8], in the absorption model with kaon exchange. Section 7, finally, contains the conclusion, partly in terms of a comparison between our results and the Ferrari-Selleri form factor approach[3,9-12].

2. CROSS-SECTION, DECAY DISTRIBUTIONS, AND HELICITY AMPLITUDES

a) General considerations

For the application of the absorption model, we have to consider the helicity amplitudes[13] for reaction (1). Let these amplitudes be denoted $\langle \lambda^*, \bar{\lambda}^* | T | \lambda, \bar{\lambda} \rangle$, where $\lambda(\bar{\lambda})$ is the helicity of the proton (anti-proton), $\lambda^*(\bar{\lambda}^*)$ the helicity of the isobar (anti-isobar).

We first list some more general properties of these amplitudes. From parity conservation one has the following symmetry relation[14]

$$\langle -\lambda^*, -\bar{\lambda}^* | T | -\lambda, -\bar{\lambda} \rangle = (-1)^n \langle \lambda^*, \bar{\lambda}^* | T | \lambda, \bar{\lambda} \rangle \qquad (3)$$

$$n = |\lambda^* - \bar{\lambda}^* - \lambda + \bar{\lambda}| \qquad (3a)$$

while charge conjugation invariance, combined with the fact that both initial and final states contain a particle and its antiparticle, implies[14]

$$\langle \bar{\lambda}^*, \lambda^* | T | \bar{\lambda}, \lambda \rangle = (-1)^n \langle \lambda^*, \bar{\lambda}^* | T | \lambda, \bar{\lambda} \rangle \ . \qquad (4)$$

These relations reduce the number of independent amplitudes from 64 to 20.

Our normalization of the helicity amplitudes is such that the differential cross-section for reaction (1), at the momentum transfer squared $-t$, is given by

$$\frac{d\sigma}{dt}(\omega, \bar{\omega}) = \frac{1}{64\pi s q^2} \times \frac{1}{4} \times \sum |\langle \lambda^*, \bar{\lambda}^* | T | \lambda, \bar{\lambda} \rangle|^2$$

where q is the c.m.s. momentum in the initial state; the sum is extended to all values of the helicities. The arguments of $d\sigma/dt$ indicate that, besides being a function of t and the total c.m.s. energy squared s, $d\sigma/dt$ also depends on the invariant mass ω of the outgoing $p-\pi^+$ pair as well as the corresponding $\bar{p}-\pi^-$ quantity $\bar{\omega}$. In fact, the differential cross-section, including the invariant mass distributions but integrated over the decay angles, is given by[15]

$$\frac{d^3\sigma}{d\omega^2 d\bar{\omega}^2 dt} = \frac{d\sigma}{dt}(\omega, \bar{\omega})\ R(\omega)\ R(\bar{\omega}) \ , \qquad (6)$$

$$R(\omega) = \frac{1}{\pi} \frac{M^* \Gamma(\omega)}{(M^{*2} - \omega^2)^2 + M^{*2} \Gamma^2(\omega)} \quad , \tag{6a}$$

where $M^* = 1237$ MeV is the mass and $\Gamma(\omega)$ is the width, depending on the invariant mass, of the isobar. In terms of the $p - N^{*++} - \pi^+$ coupling

$$G^* \, \overline{N^*_\mu} \cdot \partial_\mu N \cdot \pi \quad , \tag{7}$$

where G^* is a coupling constant of dimension inverse mass, and where the fields are denoted by the same symbols as the corresponding particles, the width is given by

$$\Gamma(\omega) = \frac{G^{*2}}{4\pi} \frac{(M + \omega)^2 - m^2}{6\omega^2} \, p^3(\omega) \tag{8}$$

where M is the proton mass, m the pion mass and

$$p(\omega) = \frac{1}{2\omega} \left[(M^2 + \omega^2 - m^2)^2 - 4M^2\omega^2 \right]^{1/2} \tag{9}$$

is the momentum of the outgoing pion in the c.m.s. of the $p - \pi^+$ pair, having invariant mass ω.

Knowing the experimental width $\Gamma(M^*) = 125$ MeV, one concludes from Eq. (8), that

$$\frac{G^{*2}}{4\pi} = 0.38 \ m^{-2} \quad . \tag{10}$$

Finally, if also the angular distribution in the decays of the isobar and the anti-isobar is considered, one has

$$\frac{d^5\sigma}{d\Omega d\bar{\Omega} d\omega^2 d\bar{\omega}^2 dt} = \frac{d^3\sigma}{d\omega^2 d\bar{\omega}^2 dt} \, W(\Omega, \bar{\Omega}) \tag{11}$$

$$\iint d\Omega d\bar{\Omega} \, W(\Omega, \bar{\Omega}) = 1 \quad . \tag{11a}$$

Here, $\Omega = (\Theta,\varphi)$ are the polar angles of the outgoing proton momentum in the isobar rest frame, conveniently referred to a co-ordinate system having z axis along the incoming proton momentum in this frame and with the x-z plane as the production plane. The anti-isobar decay angles $\bar{\Omega} = (\bar{\Theta},\bar{\varphi})$ are defined in an analogous way. The azimuthal angles φ and $\bar{\varphi}$ are equivalent to the Treiman-Yang angles[16].

The general form of the angular function $W(\Omega,\bar{\Omega})$ is given in Eq. (40) of Ref. 14). In the following we will be interested only in the special distributions

$$W_1(\Omega) = \int d\bar{\Omega}\, W(\Omega,\bar{\Omega}) =$$

$$= \frac{1}{4\pi}\left[1 + (1 - 3\cos^2\Theta)\cdot a - 2\sqrt{3}\left\{\sin 2\Theta \cos\varphi \operatorname{Re}\rho_{3,1} + \right.\right. \qquad (12)$$

$$\left.\left. + \sin^2\Theta \cos 2\varphi \operatorname{Re}\rho_{3,-1}\right\}\right]$$

$$W_2(\Theta,\bar{\Theta}) = \iint d\varphi\, d\bar{\varphi}\, W(\Omega,\bar{\Omega}) =$$

$$= \frac{1}{4}\left[1 + (1 - 3\cos^2\Theta)\cdot a + (1 - 3\cos^2\bar{\Theta})\cdot a + (1 - 3\cos^2\Theta)(1 - 3\cos^2\bar{\Theta})\cdot b\right], \qquad (13)$$

where, in the notation of Ref. 14),

$$a = \frac{1}{2} - 2\rho_{11} \qquad (14a)$$

$$b = \frac{1}{2}\left(\rho^{33}_{\underline{\underline{\ }}} - \rho^{11}_{\underline{\underline{\ }}}\right) . \qquad (14b)$$

We have used here the symmetry relation (42) of Ref. 14).

b) Cross-section and decay distribution in the Born approximation

So far the discussion has been general; we now specialize and assume that the process (1) occurs through one-pion exchange, as is illustrated by the Feynman diagram of Fig. 1. In principle, within the OMEM,

one should also consider exchange of other non-strange mesons with isotopic spin not smaller than 1, in particular the ρ meson. We suppose, however, that these contributions may be neglected, at least as a first approximation.

Using the coupling of Eq. (7), the cross-section in the Born approximation may be written[3]

$$\frac{d^3\sigma_{Born}}{d\omega^2\, d\bar{\omega}^2\, dt} = \frac{1}{16\pi^3 sq^2}\,\frac{\omega^2 p(\omega,t)}{M^*}\,\sigma_{33}(\omega,t)\,\frac{1}{(m^2-t)^2}\,\frac{\bar{\omega}^2 p(\bar{\omega},t)}{M^*}\,\sigma_{33}(\bar{\omega},t)\ , \qquad (15)$$

$$\sigma_{33}(\omega,t) = \frac{8\pi^2}{p(\omega,t)^2}\, M^*\, \Gamma(\omega,t)\, R(\omega)\ , \qquad (15a)$$

where $\Gamma(\omega,t)$ and $p(\omega,t)$ are the quantities defined in Eqs. (8) and (9), except that the square of the real pion mass m^2 is to be replaced by the "virtual pion mass" t. The quantity $\sigma_{33}(\omega,t)$ is sometimes called the "off-shell" pion-nucleon cross-section in the isotopic spin $3/2$, total angular momentum $3/2^+$ state.

The "pole approximation"[3,17] consists in substituting m^2 for t everywhere in Eq. (15), except in the propagator denominator; in particular one substitutes for $\sigma_{33}(\omega,t)$ the (theoretical or experimental) "on-shell" pion-nucleon cross-section. Because

$$\frac{\sigma_{33}(\omega,t)}{\sigma_{33}(\omega,m^2)} = \frac{p(\omega,t)^2[(M+\omega)^2-t]}{p(\omega)^2[(M+\omega)^2-m^2]}\ , \qquad (16)$$

the ratio between the two cross-sections is

$$\frac{d^3\sigma_{Born}}{d^3\sigma_{pole}} = \frac{p(\omega,t)^2\ p(\bar{\omega},t)^2[(M+\omega)^2-t][(M+\bar{\omega})^2-t]}{p(\omega)^2\ p(\bar{\omega})^2[(M+\omega)^2-m^2][(M+\bar{\omega})^2-m^2]}\ . \qquad (17)$$

This is a big factor, even for forward production; for $\omega = \bar{\omega} = M^*$, it is 8 for $-t = 0.1$ (GeV/c)^2 and 250 for $-t = 0.7$ (GeV/c)^2. This means that, while in the pole approximation the cross-section as a function of t varies like $(m^2-t)^{-2}$, in the Born approximation this variation is almost completely masked due to the t dependence of the factor (17).

For completeness it must be remarked, that often the factor of Eq. (17) is multiplied into the result of the pole approximation to give an "off-shell correction". This then means that the pole approximation, with this off-shell correction, will give essentially the same result as the Born approximation. In order to obtain the experimentally observed decrease of the cross-section with increasing momentum transfer, cut-off functions [further, theoretically derived, off-shell corrections and/or products of form factors[3,9-12]] have to be multiplied into the cross-section.

Finally, the function $W(\Omega,\bar{\Omega})$ of Eq. (11), giving the angular distribution in the decay, reads in the Born approximation

$$W_{Born}(\Omega,\bar{\Omega}) = \frac{1}{8\pi}(1+3\cos^2\Theta)\,\frac{1}{8\pi}(1+3\cos^2\bar{\Theta}) \quad . \tag{18}$$

To the extent that the real pion-nucleon elastic scattering in the neighbourhood of the N* resonance is entirely dominated by the state of total angular momentum $3/2^+$, the same distribution is also predicted by the pole approximation, with or without cut-off functions. Small admixture of other angular momentum states will cause small deviations from the form (18); however, in this approach, it always remains a product of two angular functions, one referring to the decay of the isobar, the other to the decay of the anti-isobar, implying an absence of correlation between the two decays.

c) Helicity amplitudes in the Born approximation

In writing down the helicity amplitudes $<\lambda^*,\overline{\lambda^*}|B|\lambda,\bar{\lambda}>$ for the Feynman diagram of Fig. 1[18], we denote by E and E* the energy of the incident proton and the isobar, respectively, in the total c.m.s. and by $q(q^*)$ the c.m.s. momentum in the initial (final) state. Let us further write

$$<\lambda^*,\overline{\lambda^*}|B|\lambda,\bar{\lambda}> = (-1)^{\overline{\lambda^*}+\bar{\lambda}} \cdot G^{*2} \cdot \frac{1}{2} \cdot q^2 \, J_{\lambda^*,\lambda} \, \frac{1}{m^2 - t} \, \overline{J_{\overline{\lambda^*},\bar{\lambda}}} \tag{19}$$

and also introduce the auxiliary notations

$$\eta_{\pm} = \sqrt{(E+M)(E^*+M^*)}\left[1 \pm \frac{q}{E+M} \cdot \frac{q^*}{E^*+M^*}\right] , \tag{20a}$$

$$\alpha = \frac{q^*}{E^*} \cdot \frac{E}{q} , \tag{20b}$$

$$C_{\lambda}(\vartheta) = \begin{cases} \cos \vartheta/2 \text{ for } \lambda = 1/2 \\ \sin \vartheta/2 \text{ for } \lambda = -1/2 \end{cases} . \tag{20c}$$

The quantities $J_{\lambda^*,\lambda}$ and $\overline{J_{\bar{\lambda}^*,\bar{\lambda}}}$ of Eq. (19) are then determined, as functions of the isobar production angle ϑ in the c.m.s., by the relations

$$\overline{J_{\bar{\lambda}^*,\bar{\lambda}}} = J_{\bar{\lambda}^*,\bar{\lambda}} \tag{21a}$$

$$J_{-\lambda^*,-\lambda} = (-1)^{1+\lambda^*+\lambda} J_{\lambda^*,\lambda} \tag{21b}$$

$$J_{3/2,\pm 1/2} = \eta_{\pm} \sin \vartheta \, C_{\pm 1/2}(\vartheta) \tag{21c}$$

$$J_{1/2,\pm 1/2} = \frac{1}{\sqrt{3}}\left[\mp \eta_{\pm} \sin \vartheta \, C_{\mp 1/2}(\vartheta) + \frac{E^*}{M^*} q(\cos \vartheta - \alpha) \, \eta_{\mp} \, C_{\pm 1/2}(\vartheta)\right] \tag{21d}$$

If one wants the amplitudes as functions of the invariant masses ω and $\bar{\omega}$, one has to replace M^* by ω in $J_{\lambda^*,\lambda}$ and by $\bar{\omega}$ in $\overline{J_{\bar{\lambda}^*,\bar{\lambda}}}$.

When making use of the amplitudes (19) in the absorption model calculations below, we have also made a small-angle approximation by putting $\cos \vartheta$ (and $\cos \vartheta/2$) equal to one, however always using $\cos \vartheta - \alpha = 1 - 2 \sin^2 \vartheta/2 - \alpha$, because α is in general close to 1.

3. DESCRIPTION OF THE ABSORPTION MODEL

Only the necessary formulae will be given; a complete account of the theory may be found in Ref. 2).

Consider in general a two-body production process

$$1 + 2 \to 3 + 4 \quad . \tag{22}$$

Let the helicities of particle i be denoted by λ_i, i = 1 - 4. Then the partial wave expansion of the helicity amplitudes, as functions of the production angle, reads[13)]

$$\langle \lambda_3, \lambda_4 | T | \lambda_1, \lambda_2 \rangle =$$

$$= \sum_{j=j_{min}}^{\infty} \left(j + \frac{1}{2} \right) \langle \lambda_3, \lambda_4 | T(j) | \lambda_1, \lambda_2 \rangle \, d^j_{\lambda_1 - \lambda_2, \lambda_3 - \lambda_4}(\vartheta) \approx$$

$$\approx \int_{j_{min}}^{\infty} j \, dj \, \langle \lambda_3, \lambda_4 | T(j) | \lambda_1, \lambda_2 \rangle \, J_n(2j \sin \vartheta/2) \quad . \tag{23}$$

Here, $j_{min} = \max(|\lambda_1 - \lambda_2|, |\lambda_3 - \lambda_4|)$ and $d^j_{\lambda,\mu}(\vartheta)$ are the matrix elements of the rotation operator. In Eq. (23) we have approximated the d functions by Bessel functions $J_n(2j \sin \vartheta/2)$ of order $n = |\lambda_3 - \lambda_4 - \lambda_1 + \lambda_2|$ and also converted the summation into an integration, i.e., essentially an impact parameter approximation.

The DWBA approach suggests the following expression for the partial wave helicity amplitudes[2)]

$$\langle \lambda_3, \lambda_4 | T(j) | \lambda_1, \lambda_2 \rangle = \exp[i\delta_f(j)] \langle \lambda_3, \lambda_4 | B(j) | \lambda_1, \lambda_2 \rangle \exp[i\,\delta_i(j)] \tag{24}$$

where $\langle \lambda_3, \lambda_4 | B(j) | \lambda_1, \lambda_2 \rangle$ are the partial wave helicity amplitudes in the Born approximation and $\delta_i(j)[\delta_f(j)]$ is the phase shift for the elastic scattering, assumed to be helicity non-changing, in the initial (final) state.

In order to determine the phase shifts, we also assume that the elastic scattering is purely diffractive, given by the scattering on a partially absorbing disc of radius.R. This amounts to a differential elastic cross-section, which reads

$$\frac{d\sigma_{el}}{dt} \approx \frac{\sigma_{tot}^2}{16\pi} \exp\left[\frac{1}{4} R^2 t\right] \tag{25}$$

where σ_{tot} is the total cross-section. This is usually a good approximation for small momentum transfers. One then derives

$$\exp[\, 2i\delta(j)] \approx 1 - 2A \exp[-\gamma j^2] \tag{26}$$

where we have put

$$A = \frac{\sigma_{tot}}{2\pi R^2} \tag{27a}$$

$$\gamma = \frac{2}{R^2 q^2} \quad . \tag{27b}$$

The quantity A can be thought of as the absorptivity of the disc. The model requires $2A \lesssim 1$ for consistency.

As can be seen from Eqs. (24) and (26), if $A \approx \frac{1}{2}$, the absorption model introduces a large damping of the low partial waves, remedying, at least at not too high an energy, the disease of the Born approximation to exceed the unitarity limit in these waves.

4. APPLICATION OF THE ABSORPTION MODEL TO REACTION (1)

We now feed in the helicity amplitudes (18) into the absorption model formula (23). For the so far unspecified parameters we proceed as follows.

The parameters R_i and A_i for the elastic scattering in the initial state can be determined directly from experiment[19-21]. The optical model for elastic $\bar{p}$ - p scattering gives good agreement with the data for small scattering angles. Also, the approximation of purely diffractive scattering should be especially good for proton-antiproton reactions, because the ratio X of the real to the imaginary part of the forward scattering amplitude has been measured to be less than 20%; dispersion theory predicts[22] $|X| \lesssim 5\%$ in the incident momentum range 3 - 7 GeV/c.

Numerically one finds $A_i \approx \frac{1}{2}$ all over the mentioned energy range, while the interaction radius R_i decreases slowly from about 1.5 F at 3 GeV/c to about 1.4 F at 7 GeV/c.

Lack of knowledge of the elastic scattering in the final state is substituted by the assumption that it allows the same parametrization as in the initial state. Numerically we choose $A_f = \frac{1}{2}$ and, merely to have some sort of standard, $R_f^2 = 3\, R_i^2$, corresponding to an elastic as well as a total cross-section being three times bigger than the corresponding quantities in the initial state.

Concerning the validity of the absorption version of the one-pion exchange model in the present case, we remark that due to the experimentally large annihilation region [large R_i in the optical model (25)], the range of the pion forces (pion Compton wavelength = 1.4 F) at least does not exceed the range of the residual forces. Also, the cross-section for reaction (1) is small compared to the total $\bar{p}$ - p cross-section (typically 1 - 2 mb compared to σ_{tot} around 70 mb).

In fact, it was to $\bar{p}$ - p reaction that Sopkovich first applied the absorption model[5], and when it was rediscovered by Chiu and Durand[6], they also applied it to $\bar{p}$ - p reactions, among them reaction (1), at first, however, without taking proper account of the spins.

5. COMPARISON WITH EXPERIMENT FOR REACTION (1)

a) Cross-section

The result of our calculations of the cross-section for reaction (1) is compared to the experimental data[10] at 3.6 and 5.7 GeV/c in Fig. 2 on a logarithmic scale. In this diagram we have also plotted the cross-section, as determined from the unmodified Born approximation according to formula (15), without any form factor. All theoretical curves are calculated without taking into account the finite width of the isobars.

The Born approximation cross-section is too big compared with the experimental ones by a factor of around 15 in the forward direction, and does not give the sufficient decrease with increasing momentum transfer; the main reason for this is the ratio (17). In order to bring it into agreement with experiment, one has to introduce a cut-off function $F(t)^2$ into the cross-section. One possible form of $F(t)$ is

$$F(t) = F(0) \exp(t/a) \tag{28}$$

$$F(0) = 0.33 \tag{28a}$$

$$a = 26\ m_\pi^2 \ . \tag{28b}$$

Another possible form is suggested by the work on p p collision by Ferrari and Selleri[3,9-12]; still another form factor is used in Ref. 10). A direct comparison of these results with ours is, however, not possible, because there the finite width of the isobars is taken into account.

The curves calculated in the absorption model are still too big in absolute magnitude by a factor of about 5[23], but they reproduce rather well the variation with t. To see this in more detail we have in Fig. 3, on a linear scale, plotted the experimental results at 3.6 GeV/c, the result of the unmodified Born approximation multiplied by the cut-off function (28) and one-fifth of the result of the absorption model.

Concerning the dependence of the absorption model results on the choice of the absorption parameter R_f we remark that choosing a somewhat smaller value than $\sqrt{3}\ R_i$ will give a larger cross-section, but will not change either the slope of the cross-section or the predicted decay distributions.

The energy variation of the total cross-section for reaction (1) is shown in Fig. 4; all the experimental points[10-12] are for the invariant masses ω and $\bar{\omega}$ between 1.13 and 1.33 GeV. The theoretical curve is one-fifth of the result of our calculations within the absorption model. As can be seen, this curve behaves roughly as $s^{-1} q^{-2}$. This can be understood from the observation that if the absorption parameters R and A are independent of energy, the impact parameter expansion in Eq. (23) always gives the same energy dependence to the helicity amplitudes in the unmodified as in the absorption OMEM, which in the present case (i.e., pion exchange) means a cross-section behaving like $s^{-1} q^{-2}$, from Eq. (5). The slight deviation from this behaviour is explained by the variation of R_i (and R_f) with energy.

For comparison, in Fig. 4 we have also plotted the experimental ratio η of the cross-section for reaction (1), with the above-mentioned restriction on the invariant masses, to the total cross-section for production of $\bar{p}\pi^- p\pi^+$; while this latter stays about constant over the momentum range 3.25 to 7 GeV/c (it varies between about 3.5 mb and about 3.0 mb), the ratio η decreases from about 65% to about 35% over the corresponding range, thus accounting almost completely for the decrease with energy of the cross-section for reaction (1).

b) Decay distributions

The decay parameters ρ_{ik} of Eqs. (12) to (14) have been measured as functions of the momentum transfer at 3.6 and at 5.7 GeV/c; the comparison between these experimental results and the predictions from our calculations is shown in Fig. 5. Remembering, that in the unmodified one-pion exchange model, with or without form factor, the predictions are $\rho_{11} = 0.5$, $\rho_{3,1} = \rho_{3,-1} = 0$, one concludes that the suppression of the low partial waves in the absorption model changes the decay distributions to be in much better agreement with the data, in particular at 5.7 GeV/c. Even if background effects could be invoked to explain some discrepancy between, for example, the value 0.5 for ρ_{11} and the experimental ones, we think it is rather difficult to explain such large deviations as those observed, and especially to reproduce the dependence on the momentum transfer.

We have also calculated those combinations of the joint spin density matrix elements which enter into the joint decay distribution $W(\Omega,\bar{\Omega})$ of Eq. (11). At an incident momentum of 3.6 GeV/c we find in particular for the parameters in the distribution $W_2(\Theta,\bar{\Theta})$ of Eq. (13), averaged over the production angle: $a = -0.29$ (corresponding to $\rho_{11} = 0.40$) and $b = 0.15$. Almost the same values are obtained at 3.25 GeV/c.

As can be seen from Eq. (13), the condition for a correlation between the decay of the isobar and the anti-isobar to show up in the $\Theta - \bar{\Theta}$ distribution is $b - a^2 \neq 0$. Our theoretical prediction is $b - a^2 = 0.05$[24], i.e., a small correlation of this type.

The corresponding experimental values at 3.6 GeV/c[25], averaged over $0.0\ (\mathrm{GeV/c})^2 \leq -t \leq 0.4\ (\mathrm{GeV/c})^2$, are $a = -0.29 \pm 0.13$ (i.e., $\rho_{11} = 0.40 \pm 0.07$) and $b = 0.41 \pm 0.13$, giving $b - a^2 = 0.32 \pm 0.16$. From a sample of events at 3.28 and 3.69 GeV/c, unrestricted with respect to momentum transfer, it was found[26] that $a = -0.22 \pm 0.03$ (giving $\rho_{11} = 0.36 \pm 0.02$) and $b = 0.23 \pm 0.06$, implying $b - a^2 = 0.18 \pm 0.07$. Thus in both cases there is found experimentally a small correlation in the decay of the isobars, which is in decent agreement with the predictions from our calculations.

6. APPLICATION TO REACTION (2)

Although we have formulated the theory so far for reaction (1), it can with minor changes also be applied to kaon exchange in reaction (2). Besides trivial replacements, the only change will be in the determination of the coupling constant: while the $p - N^* - \pi$ coupling constant can be expressed directly in the width of the isobar, the decay of Y* into a nucleon and a kaon is energetically forbidden. We may obtain an estimate of this coupling constant from supposed SU_3 invariance:

$$\frac{G^2_{pY^*K}}{4\pi} = \frac{3}{2}\,\frac{G^2_{\Lambda Y^*\pi}}{4\pi} \approx 4.2\ m_K^{-2}\ . \qquad (28)$$

However, such an estimate is very uncertain, due to the large mass difference between the pion and the kaon. Anyhow, using this value, we arrive at a total cross-section for reaction (2) at 5.7 GeV/c incident momentum of 16 mb. The experimental value is about 5 μb[27]. In order to reproduce this, one needs in our model

$$\frac{G^2_{pY^*K}}{4\pi} \approx 0.08\ m_K^{-2}\ . \qquad (29)$$

Taking the point of view that the predicted cross-section for reaction (2) should again, as in the case of reaction (1), be about a factor of 5 bigger than the experimental one, this coupling constant should instead be $0.18\ m_K^{-2}$. This value of the N-Y*-K coupling constant could, in principle, be tested in the reaction $Kp \to \rho Y^*$, also assuming here kaon exchange.

7. CONCLUSIONS

From the preceding sections we conclude that the absorption version of the one-pion exchange model for reaction (1) is able to account for the slope of the differential and the energy variation of the integrated cross-section and for the decay distributions, including a small correlation between the decays of the isobar and the anti-isobar. Only the absolute value of the cross-section comes out a factor of five too big, a feature which occurs also in the absorption model treatment of other reactions, in which particles with high spins are produced[28].

The success of our approach to predict the decay distributions correctly is an argument in favour of the absorption model versus the form factor version of the one-pion exchange model. However, we would like to point out that this feature seems to be common to all models which "unitarize" the Born approximation, i.e., suppressing the low partial waves leaving the higher ones essentially unchanged[29]. In order to judge between different unitarized theories, one would then need experiment with much better statistics or to find some other distinguising feature.

The reaction (1), or more generally the process $\bar{p}p \to \bar{p}\pi^- p\pi^+$ has previously mostly been compared to the Ferrari-Selleri theory, taken over unchanged from proton-proton collisions. It has been shown that this model gives good agreement with the data in the range 3.25 to 7 GeV/c incident momentum, except concerning the decay distributions; restricting the theory to reaction (1), the Ferrari-Selleri model predicts the same decay distributions as the pole approximation.

A detailed comparison between our calculations and the Ferrari-Selleri approach is however difficult, mainly because we have here neglected the finite width of the isobar. Let us only remark that the invariant mass spectrum, successfully predicted in the Ferrari-Selleri model, is in shape in fair agreement also with our approach. This is so, simply because from our calculations we find that $d\sigma/dt(\omega,\bar{\omega})$ does not depend significantly on the invariant masses, implying that the invariant mass distribution is given by the factor $R(\omega)\ R(\bar{\omega})$, from Eq. (6), in rough agreement with the data.

ACKNOWLEDGEMENTS

We want to thank Dr R. Keyser for invaluable help in the numerical calculations, Dr E. Ferrari for many useful comments, and Drs E. Lohrmann, T. Ferbel and A. Cooper for discussions on the experimental data and for communication of unpublished experimental results.

REFERENCES AND FOOTNOTES

1) For a recent review of the OMEM, including references to earlier work, see:
J.D. Jackson, invited paper at the Topical Conference on Correlation of Particles Emitted in Nuclear Reactions, Gatlinburg, Tennessee, October 15-17, 1964, an elaborate version of which is to be published in Revs.Mod.Phys.

2) K. Gottfried and J.D. Jackson, Nuovo Cimento 34, 735 (1964).

3) E. Ferrari and F. Selleri, Suppl. Nuovo Cimento 24, 453 (1962) and Nuovo Cimento 27, 1450 (1963).

4) J.D. Jackson and H. Pilkuhn, Nuovo Cimento 33, 906 (1964) and errata, Nuovo Cimento 34, 1841 (1964).

5) N.J. Sopkovich, Nuovo Cimento 26, 186 (1962).

6) L. Durand and Y.T. Chiu, Phys.Rev. Letters 12, 399 (1964) and erratum, Phys.Rev. Letters 13, 45 (1964).

7) K. Dietz and H. Pilkuhn, CERN preprint 10013/TH 450 (1964), to be published in Nuovo Cimento.

8) A.H. Rosenfeld, A. Barbaro-Galtieri, W.H. Barkas, P.L. Bastien, J. Kirz and M. Roos, Revs.Mod.Phys. 36, 977 (1964).

9) H.C. Dehne, E. Lohrmann, E. Raubold, P. Söding, M.W. Teucher and G. Wolf, Phys.Rev. 136, B 843 (1964).

10) K. Böckmann, B. Nellen, E. Paul, I. Borecka, J. Diaz, U. Heeren, U. Libermeister, E. Lohrmann, E. Raubold, P. Söding, S. Wolff, S. Coletti, J. Kidd, L. Mandelli, V. Pelosi, S. Ratti, and L. Tallone, Phys.Letters 15, 356 (1965).

11) T. Ferbel, A. Firestone, J. Sandweiss, H.D. Taft, M. Gailloud, T.W. Morris and W.J. Willis, BNL 8814, submitted to Phys.Rev.

12) T. Ferbel, A. Firestone, J. Johnson, J. Sandweiss and H.D. Taft, preprint, submitted to Phys. Letters.

13) M. Jacob and G.C. Wick, Ann.Phys. 7, 404 (1959).

14) H. Pilkuhn and B.E.Y. Svensson, CERN preprint 65/35/5/TH 510 (1965) to be published in Nuovo Cimento.

15) J.D. Jackson, Nuovo Cimento 34, 1644 (1964) and references cited therein.

16) S.B. Treiman and C.N. Yang, Phys.Rev. Letters 8, 140 (1962).

17) F. Salzman and G. Salzman, Phys.Rev. 125, 1703 (1962).

18) We learned from Dr E. Lohrmann, that the helicity amplitudes (19) have also been derived, in a form suitable for application of the absorption model, by G. Ebel.

19) W. Galbraith, E.W. Jenkins, T.F. Kycia, B.A. Leontić, R.H. Phillips and A.L. Read, BNL 8744.

20) O. Czyzewski, B. Escoubès, Y. Goldschmidt-Clermont, M. Guinea-Moorhead, D.R.O. Morrison and S. de Unamono-Escoubès, Phys. Letters 15, 188 (1965).

21) T. Ferbel, A. Firestone, J. Sandweiss, H.D. Taft, M. Gailloud, T.W. Morris, A.H. Bachman, P. Baumel and R.M. Lea, Phys.Rev. (to be published).

22) P. Söding, Phys. Letters 8, 285 (1964).

23) We have estimated the reduction factor due to the finite width of the isobars to be about 0.5 in the present case, but have not included it in the theoretical predictions.

24) This value is, incidentally, obtained at all production angles.

25) Private communication from E. Lohrmann and S. Wolff.

26) Private communication from T. Ferbel.

27) Private communication from A. Cooper.

28) One example is the reaction $K^+p \to K^*N^*$, treated in J.D. Jackson, J.T. Donohue, K. Gottfried, R. Keyser and B.E.Y. Svensson, preprint, submitted to Phys.Rev.

29) In the treatment of K^+p reactions using the K-matrix method[7], one obtains results for the spin density matrices very similar to those of the absorption model (private communication from H. Pilkuhn).

FIGURE CAPTIONS

Figure 1 : Feynman diagram for one-pion exchange in reaction (1).

Figure 2 : Cross-section for reaction (1) as function of momentum transfer on a logarithmic scale. The curves (a) are obtained from the formula (15), while the curves (b) are the absorption model results, all neglecting the finite width of the isobars. The experimental results are from Ref. 10). Vertical dotted lines indicate lower limit on $-t$ for a sharp isobar mass of 1237 MeV; experimental values below these limits have been added to the first "allowed" interval as indicated by the dotted part of the histograms.

Figure 3 : Cross-section for reaction (1) as function of momentum transfer on a linear scale. The curve (a) is the Born cross-section (15) corrected by the form factor (28), curve (b) is one-fifth of the absorption model result. Experimental results are from Ref. 10). Vertical dotted line and dotted part of the histogram have the same meaning as in Fig. 2.

Figure 4 : Integrated cross-section for reaction (1) as function of energy. The curve marked (a) is proportional to $s^{-1} q^{-2}$, the curve (b) is the one-fifth of the absorption model results. Experimental points at 3.6 and 5.7 GeV/c are from Ref. 10), while the one at 7 GeV/c is inferred from the invariant mass plot of Ref. 12), the one at 3.5 GeV/c inferred from the invariant mass plot of the combined 3.28 and 3.69 GeV/c events of Ref. 11). The open circles are the corresponding values of η, the ratio of the cross-section for reaction (1) to the cross-section for reaction $\bar{p}p \to \bar{p}\pi^- p\pi^+$.

Figure 5 : Spin space density matrix elements, giving the decay distribution (12). Experimental values are from Ref. 10); the curves are the absorption model results. Dotted vertical lines have the same meaning as in Fig. 2. Dotted experimental points at 3.6 GeV/c indicate values based on a small number of events.

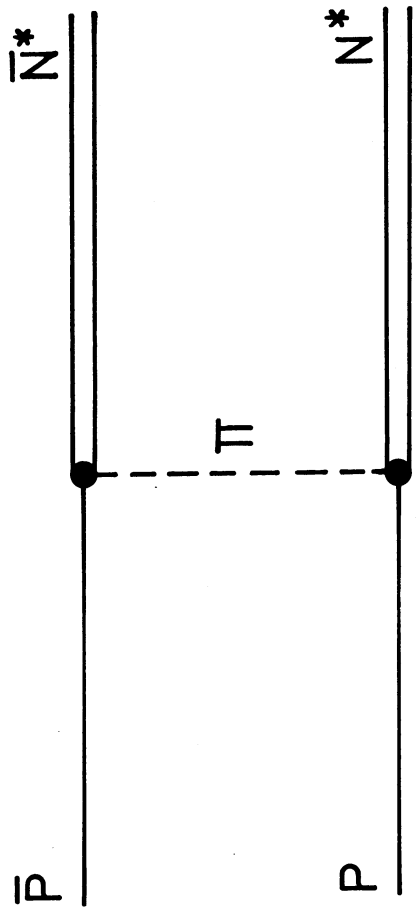

FIG.1

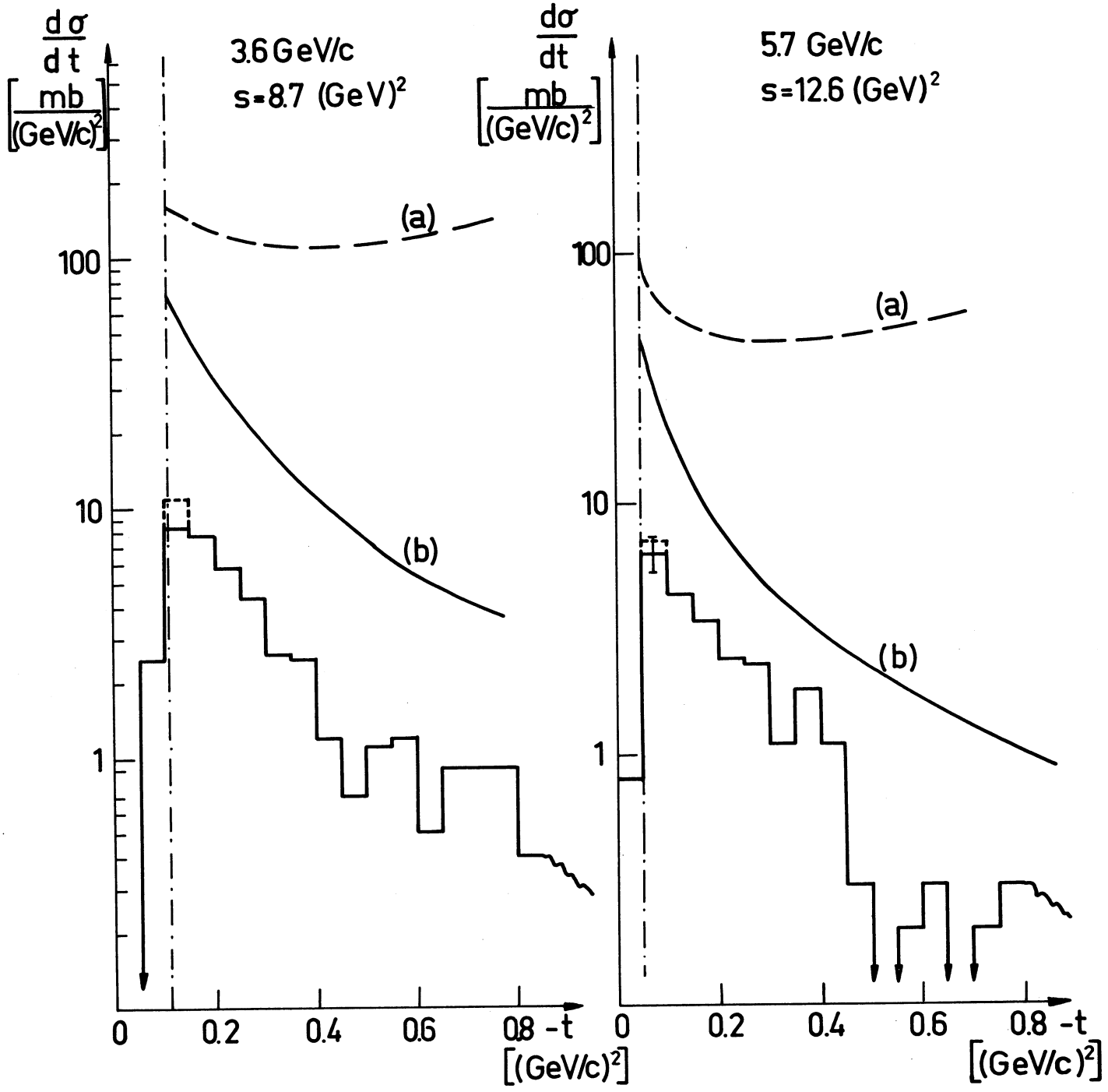
dσ/dt [mb/(GeV/c)²]
3.6 GeV/c
s=8.7 (GeV)²
(a)
(b)
100
10
1
0
0.2
0.4
0.6
0.8
-t [(GeV/c)²]
dσ/dt [mb/(GeV/c)²]
5.7 GeV/c
s=12.6 (GeV)²
(a)
(b)
100
10
1
0
0.2
0.4
0.6
0.8
-t [(GeV/c)²]

FIG. 2

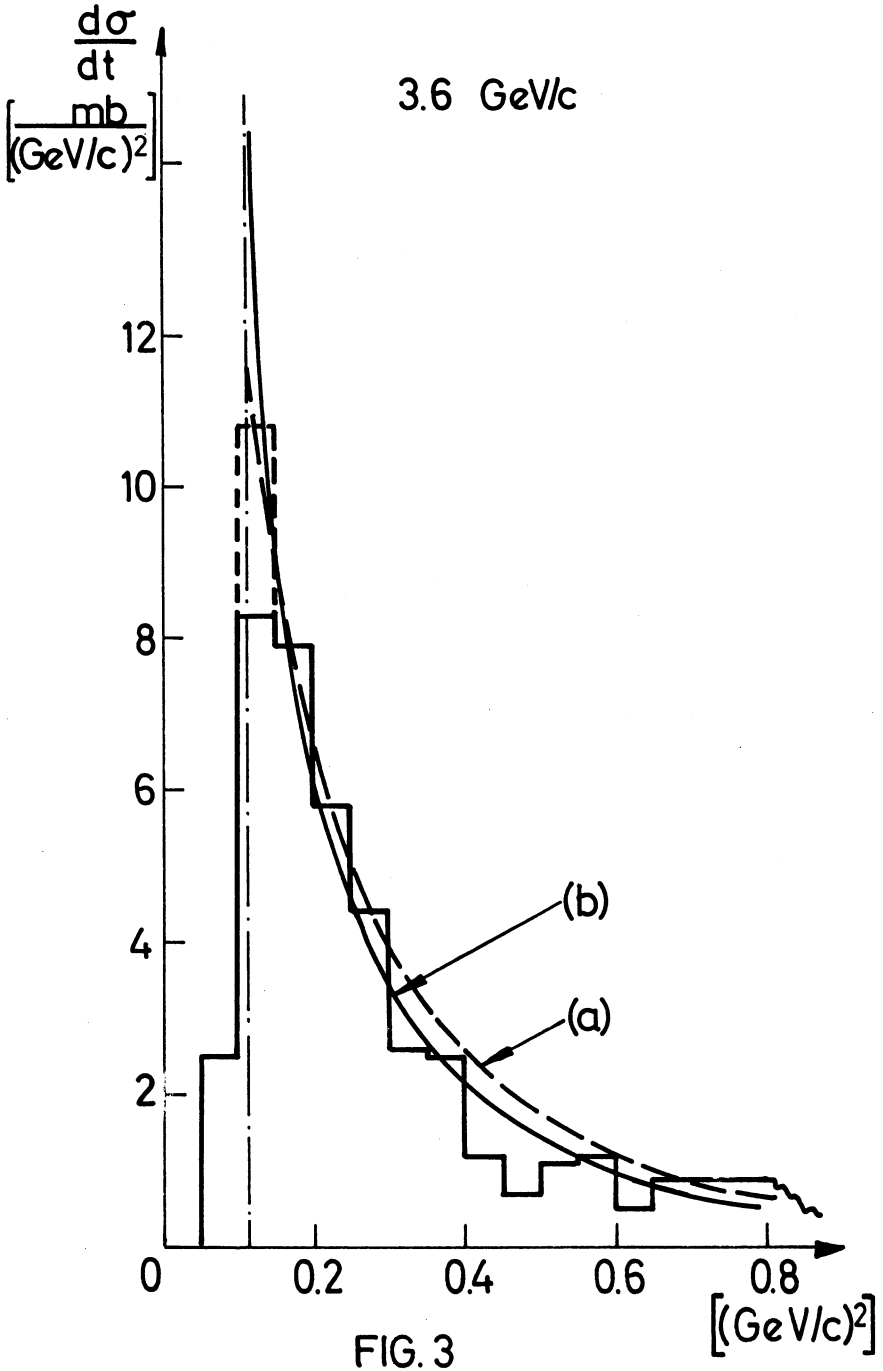
dσ/dt
[mb/(GeV/c)²]
3.6 GeV/c
12
10
8
6
4
2
0
0.2
0.4
0.6
0.8
[(GeV/c)²]
(b)
(a)

FIG. 3

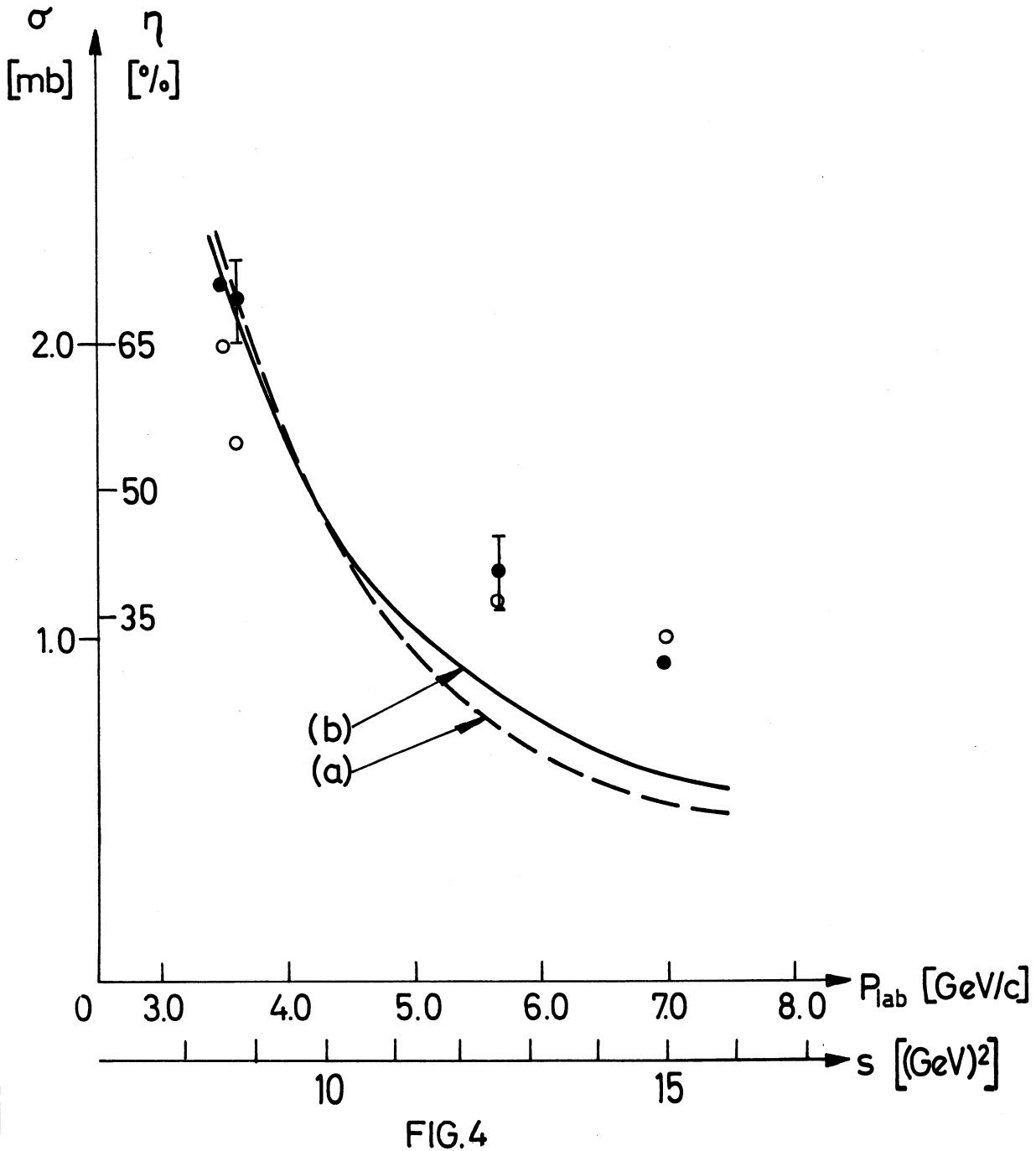
σ
[mb]
η
[%]
2.0
1.0
65
50
35
(b)
(a)
0
3.0
4.0
5.0
6.0
7.0
8.0
P_lab [GeV/c]
10
15
s [(GeV)²]

FIG. 4

Decay parameters

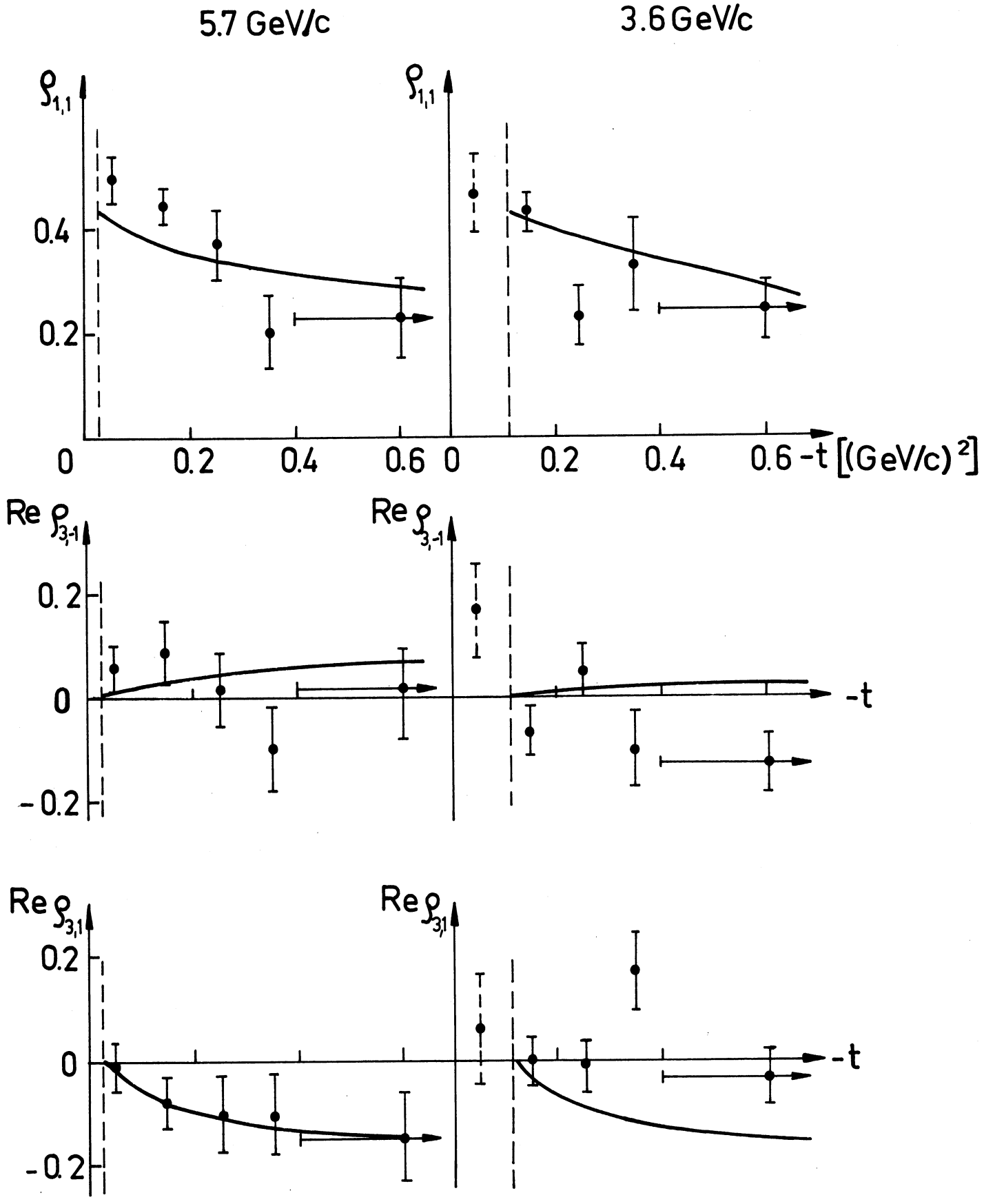

FIG.5